A Closed-Form Solution for Coarse Registration of Point Clouds Using Linear Features

Fangning He, Ph.D., S.M.ASCE[1]; and Ayman Habib[2]

Abstract: This paper presents a closed-form procedure for the coarse registration of three-dimensional (3D) point clouds using automatically extracted linear features, which have been manually matched. Corresponding linear features are defined by nonconjugate endpoints that do not necessarily define compatible direction vectors. Because the point clouds could be derived from different sources (e.g., laser scanning data sets and/or photogrammetric point clouds that are referenced to arbitrary reference frames), the proposed procedure estimates the scale, shift, and rotation parameters that relate the reference frames of these data sets. The proposed approach starts with a quaternion-based procedure for initial estimation of the transformation parameters using the minimal number of required conjugate line pairs (i.e., two noncoplanar linear features from each point cloud). The initial estimate of the transformation parameters is then used to ensure the compatibility of the direction vectors of the involved linear features. The modified direction vectors together with the endpoints of the linear features are used for deriving a better estimate of the transformation parameters. Experimental results from both simulated and real data sets verified the feasibility of the proposed procedure in providing good quality for the approximate parameters of the transformation parameters for point-based fine registration procedures. **DOI: 10.1061/(ASCE)SU.1943-5428.0000174.** © *2016 American Society of Civil Engineers.*

Introduction

Over the last decade, there has been an increasing demand for the utilization of three-dimensional (3D) models in various applications, such as industrial site modeling, 3D documentation of historical monuments, urban planning, telecommunications, and different civilian and military needs. Currently, 3D reconstruction/representation of objects of interest can be achieved through either active or passive remote sensing systems. Active sensors, such as laser scanners, directly provide precise and dense point cloud, which is properly scaled, along the scanned objects. In spite of the high point density of laser scanning data, break lines are not usually well defined by such data. Moreover, the derived point cloud usually lacks spectral information (especially when dealing with data collected by laser scanners onboard mobile platforms). On the other hand, passive sensors, such as digital frame cameras, can be incorporated for 3D reconstruction while providing spectral attributes for the derived coordinates. Such semantic attributes would allow for the derivation of better and more reliable information pertaining to the reconstructed objects. Moreover, the images can be used for accurate derivation of break lines. However, the main challenge in deriving 3D information from passive sensors is feature matching in overlapping imagery (i.e., the automated identification of conjugate features in the involved images). Given the abovementioned characteristics of derived 3D point clouds from active and passive sensors, the research and professional communities have advocated the integration of point clouds from these data-acquisition modalities (González-Aguilera et al. 2009). Effective integration of derived data from these modalities is contingent on their alignment relative to a common reference frame, which is known as the registration problem.

According to Habib and Alruzouq (2004), a comprehensive registration procedure should address four issues: (1) the transformation parameters that relate the reference frames of the involved data sets; (2) the registration primitives, which are the conjugate features that can be identified from the different data sets and used for the estimation of transformation parameters; (3) the similarity measure, which is the mathematical constraint that describes the coincidence of conjugate features after the registration process; and (4) the matching strategy, which represents the controlling framework for the automatic registration process. To date, there has been an extensive body of research for the registration of derived data sets from passive and active sensors. In this regard, two different approaches can be adopted for the registration of two-dimensional (2D) image-based and 3D laser point clouds. The first approach is based on a 2D-to-3D alignment strategy, in which the registration is achieved using identified features in the 2D images and 3D point cloud in question (Ding et al. 2008; Habib et al. 2004; Mastin et al. 2009). Automated identification of corresponding features in 2D and 3D data sets is quite difficult. The second approach is based on a 3D-to-3D registration strategy. More specifically, a point cloud can be generated from 2D imagery through the automated identification of conjugate points in overlapping imagery. Then the registration problem is solved through the alignment of the image-based and laser scan point clouds. The generation of a 3D point cloud from 2D images can be achieved through one of two strategies. In the first strategy, the interior orientation parameters (IOPs) of the utilized camera as well as the exterior orientation parameters (EOPs) of the involved imagery are assumed to be known. The IOPs of the utilized camera can be obtained through a camera calibration exercise. The EOPs, on the other hand, can be derived through either a direct or indirect georeferencing procedure. Following the estimation of IOPs and EOPs, conjugate points are identified in the overlapping images using image matching techniques. Then, the image coordinates of conjugate points are manipulated through a simple intersection procedure using the available

[1]Student, Lyles School of Civil Engineering, Purdue Univ., West Lafayette, IN 47906 (corresponding author). E-mail: he270@purdue.edu

[2]Professor, Lyles School of Civil Engineering, Purdue Univ., West Lafayette, IN 47906. E-mail: ahabib@purdue.edu

Note. This manuscript was submitted on November 30, 2014; approved on November 23, 2015; published online on February 3, 2016. Discussion period open until July 3, 2016; separate discussions must be submitted for individual papers. This paper is part of the ***Journal of Surveying Engineering***, © ASCE, ISSN 0733-9453.

IOPs and EOPs for the derivation of the 3D coordinates of the corresponding object points (Kraus 2007). The second strategy is introduced by the computer vision community and is known as structure from motion (SfM). This strategy simultaneously estimates the EOPs of the involved images and drives the 3D coordinates of corresponding features in those images (Huang and Netravali 1994). In the absence of control information, SfM-based point clouds are usually referred to an arbitrary reference frame. It can be argued that 3D-to-3D registration approach has several advantages: (1) automated identification of conjugate features in 2D images and 3D point clouds is more complex and less reliable than the identification of conjugate features in 3D data sets; (2) modern dense image-matching techniques, such as the semiglobal image matching (Hirschmuller 2005), are capable of generating 3D point clouds from imagery with large overlap and side lap ratios; and (3) 3D-to-3D registration is more general, because it can be used for the registration of any 3D data sets regardless of their origin (e.g., image-based and/or laser scanning data derived from terrestrial and/or airborne platforms). Therefore, this research is focusing on 3D-to-3D data registration.

The registration of 3D data sets involves the estimation of the 3D Helmert transformation parameters (i.e., scale factor, three translations, and three rotation angles) relating the reference frames of the different point clouds. When dealing with two point clouds that have been captured by well-calibrated laser scanners, the scale factor does not have to be estimated, because it is implicitly defined by the measured ranges (Al-Durgham and Habib 2014). To derive the 3D Helmert transformation parameters, either a closed-form or nonclosed-form solution can be adopted. Different from the conventional approach (Slama et al. 1980; Wolf and Dewitt 2000), which is based on a nonlinear least-squares solution, the closed-form solution does not require initial approximate values for the unknown transformation parameters (Horn 1987). Depending on the accuracy of the estimated transformation parameters, registration procedures could be classified as either coarse or fine registration techniques (Matabosch et al. 2005). Coarse registration techniques are usually used to establish rough alignment between the involved point clouds. Fine registration, on the other hand, starts from coarsely aligned point clouds to achieve more precise alignment of the involved data sets.

The registration primitives could be points, lines, or planar features. The point-based registration could be using point targets, individual points within the data, or key points that have characteristic attributes. Target-based registration uses artificial targets, which are set up within the field of view of the data-acquisition systems and designed to facilitate their automatic identification from the derived point clouds. Using targets requires careful manual interaction to make sure that the setup targets are capable of providing precise estimate of the transformation parameters (e.g., ensuring that the targets are well distributed within the collected data). Site accessibility as well as safety issues might limit the use of targets as the registration primitives. Moreover, targets might not be the appropriate primitives for the registration of data sets that are acquired at different times, because one cannot guarantee that the targets are set up at the same locations. Other point-based procedures use the entirety of the available points within the data sets to estimate the transformation parameters relating these data sets. The iterative closest point (ICP) is an example of the most commonly used procedure in this category (Besl and McKay 1992) in which the transformation parameters are iteratively refined by generating pairs of corresponding points and minimizing point-to-point distances. Because of the irregular nature of point clouds, point-to-point correspondence cannot be always assumed. Therefore, different variants of the ICP have been introduced for such situations. For example, the iterative closest patch (ICPatch) uses points in one point cloud and triangular patches in another point cloud as the registration primitives (Habib et al. 2010). Instead of minimizing the point-to-point distance, the ICPatch algorithm is implemented by minimizing the sum of the squared normal distances between conjugate point-to-patch pairs. An evaluation of various variants of the ICP has been conducted by Rusinkiewicz and Levoy (2001). In their paper, the classical ICP algorithm was assumed to be composed of six different stages. Then, the ICP variants were classified into different categories as modification to one or more of these stages. The ICP and its variants have been proven to be accurate (i.e., they constitute the bulk of fine registration approaches). However, these approaches require an initial rough alignment of the involved point clouds to establish the correspondence between a point in one point cloud and its nearest point in the other one. Key-point–based registration starts with applying detectors that identify point features with multiple descriptors. The detected points in the involved point clouds are then matched using their descriptors (e.g., the distance between the descriptor attributes of these points). Kim and Hilton (2013) investigated the performance of four different key-point–based registration approaches, such as spin images, 3D shape context (SC), signature of histograms of orientations (SHOTs), and fast point feature histograms (FPFHs). Chen et al. (1998) proposed a *RANSAC* (Fischler and Bolles 1981)-based exhaustive search method for identifying corresponding key points, which are then used for the alignment process. The key-point–based registration techniques are usually time-consuming, because the key-point extraction and matching processes are computationally expensive.

Linear and planar features have been repeatedly used as registration primitives for coarse alignment of point clouds. Jaw and Chuang (2008) introduced a mathematical model for line-based and plane-based point cloud registration. Experimental results from this work showed that linear and planar primitives yield reliable estimates of the transformation parameters. Stamos and Leordeanu (2003) used fitted planes and their intersections for the registration of two laser scans. This approach would fail if the involved scenes do not contain a sufficient number of 3D lines and planes. Yao et al. (2010) developed a *RANSAC*-based algorithm to register laser scans in a pairwise fashion, in which groups of linear and planar features are used as the registration primitives. However, this algorithm is sensitive to the presence of repetitive patterns and the registration of outdoor scenes usually failed. Al-Durgham and Habib (2014) proposed an association-matrix–based sample consensus approach for the registration of terrestrial laser scans using linear features. It has been demonstrated that compared with the traditional *RANSAC* algorithm, the association-matrix–based approach is capable of producing more correct results in fewer trials. Their approach is based on a nonlinear solution for the transformation parameters while assuming a unit scale factor. Han (2010) proposed a noniterative solution to estimate similarity or affine transformation parameters using vector geometry from hybrid geometric features (including points, lines, and planes). By performing a numerical analysis, the author has demonstrated that the estimated transformation parameters through the proposed approach are at the same level of quality when using the classic least-squares approach, but with an improved computational performance in real-field applications. Additional improvement of this approach is conducted by Han and Jaw (2013). Along with hybrid geometric features, the improved approach uses point clusters to estimate the transformation parameters. Thus, it is capable of providing a more flexible parameter estimation when dealing with similarity transformation models. However, this approach assumes compatible directions of utilized

vectors. In addition to linear and planar features, circular and spherical features have been investigated. For example, Chen and Stamos (2006) proposed the use of circular features, and Franaszek et al. (2009) used locally fitted 3D spheres. However, both circular and spherical features are only available in some specific scenes. Comparing the different types of features that could be used for point cloud registration, one can argue that linear features are more convenient for the following reasons (Al-Durgham and Habib 2014): (1) linear features are the most common primitives that would exit in both indoor and outdoor scenes, such as urban scenes and industrial sites; (2) the linear feature representation scheme could be easily chosen to simplify the registration process; (3) linear features can be identified in photogrammetric and laser data; and (4) compared to planar features, fewer lines are required for the registration process.

The objective of this research is the development of a closed-form procedure for coarse registration of point clouds that are derived from either active or passive imaging sensors using linear features. To illustrate the proposed procedure, the paper starts with the utilized approaches for point cloud generation from overlapping images and the automated derivation of linear features. Then, the mathematical details for using manually identified conjugate linear features for closed-form estimation of the transformation parameters are discussed. Experimental results using both simulated and real data sets are then presented. Finally, the paper introduces the drawn conclusions as well as the recommendations for future work.

Methodology

In this paper a closed-form approach is developed for the coarse registration of point clouds that are derived from either active or passive imaging sensors. The developed approach has the following characteristics: (1) it is based on manually identified conjugate linear features, which have been automatically extracted from the point clouds; (2) conjugate linear features are defined by noncorresponding endpoints that do not necessarily define compatible directions; and (3) the proposed procedure does not require initial values for the transformation parameters (shifts, rotation angles, and scale) relating the reference frames for the point clouds.

Image-Based Point Cloud Generation

Passive sensors, mainly in the form of digital frame camera, still remain the most complete, economical, flexible, and widely used approach for the generation of a point cloud from acquired images (Remondino and El-Hakim 2006). In this research, a two-step procedure is adopted for the image-based point cloud generation process. In the first step, a fully automated approach, which was developed by He and Habib (2014), is used for the recovery of the EOPs of the acquired images. This approach starts with a linear approach for the estimation of the relative orientation parameters (ROPs) relating all the stereo pairs within the available images using Scale-Invariant Feature Transform (SIFT)-based conjugate points. The ROPs are then used in an incremental augmentation approach for evaluating the EOPs of the imagery in a local coordinate system. In this regard, it should be noted that the position, orientation, and scale of the established reference frame depends on the seed image triplet used in the image augmentation process. In the second step, the semiglobal dense matching algorithm (Gehrke et al. 2010; Hirschmuller 2005) is implemented to generate a dense point cloud.

Linear Feature Extraction

One of two approaches can be used for the derivation of 3D linear features from the image-based and laser scanning point clouds:

1. Linear features can be indirectly derived through planar feature segmentation and intersection of neighboring planes (Lari et al. 2011). Because the intersection procedure provides infinite lines, the endpoints of the linear features are established through projection of the point cloud within a given buffer around the derived intersection onto the infinite linear feature.
2. Linear features can be directly derived from point clouds. In this work, a region-growing approach is used (Lari and Habib 2013). Principal component analysis (PCA) is used to identify seed regions that belong to potential linear features. Then, neighboring points that belong to the same feature are sequentially identified/incorporated by examining the normal distance between those points and the mathematical model associated with the seed regions.

Using either one of these approaches, the automatically extracted linear features are represented by their endpoints. In this research, conjugate linear features are manually identified. In this regard, it should be noted that the endpoints representing conjugate linear features are not corresponding to each other and do not necessarily define compatible direction vectors. The next section provides the mathematical details for deriving the transformation parameters using such linear features.

Estimation of Transformation Parameters

The underlying conceptual basis of the developed procedure can be summarized as follows:

1. The rotation matrix relating the reference frames of the two point clouds is estimated first using a quaternion-based closed-form solution; and
2. The scale and shift parameters are then estimated using a linear mathematical model based on a modified weight matrix.

Derivation of the Rotation Matrix

The conceptual basis of the developed approach for estimating the rotation matrix starts with the introduced quaternions procedure by Horn (1987) and Guan and Zhang (2011). The proposed approach in these publications assumes that the direction vectors of conjugate linear features in two data sets are parallel after applying the rotation matrix relating the reference frames of these data sets. This parallelism can be mathematically represented by Eq. (1)

$$n_i^2 = \lambda_i \, \boldsymbol{R}_1^2 \, n_i^1 \tag{1}$$

where n_i^1 is the direction vector of the ith linear feature in the first point cloud; n_i^2 is the direction vector of the corresponding linear feature in the second point cloud; $\boldsymbol{R}_1^2$ is the rotation matrix relating the reference frames of the first and second point clouds; and λ_i is a scale factor.

Assuming that the direction vectors (n_i^1 and n_i^2) are unit vectors, the scale factor (λ_i) will be ± 1. The plus sign should be used when the two direction vectors are compatible (i.e., the two direction vectors are pointing in the same direction after applying the rotation matrix); otherwise, the negative sign should be used. The next two subsections will introduce the quaternion-based closed-form solution for the direct estimation of the rotation matrix when dealing with compatible and incompatible direction vectors. In this regard,

one should note that the proposed approach for dealing with compatible direction vectors is identical to the one proposed by Horn (1987) and Guan and Zhang (2011) and is only included in this paper to emphasize the difference when dealing with incompatible direction vectors as well as justifying the logic behind the developed methodology.

Estimating the Rotation Matrix When Dealing with Compatible Direction Vectors

As already mentioned, when dealing with one pair of conjugate linear features with compatible directions, one can introduce the constraint in Eq. (2) while considering the random errors associated with the available direction vectors

$$n_i^2 = \boldsymbol{R}_1^2\ n_i^1 + \ e_i \tag{2}$$

where n_i^1 and n_i^2 are unit direction vectors; and e_i is the misalignment error associated with the conjugate pair for the ith linear feature. Assuming there is a set of n conjugate linear features, there can be n sets of equations of the form in Eq. (2). To estimate the unknown rotation matrix $\boldsymbol{R}_1^2$, the least-squares adjustment is used to minimize the sum of squared errors (SSE) for all the involved n conjugate linear features, as shown in Eq. (3)

$$\begin{aligned}\min_{R_1^2} \sum_{i=1}^{n} e_i^T e_i &= \min_{R_1^2} \sum_{i=1}^{n} (n_i^2 - \boldsymbol{R}_1^2\ n_i^1)^T (n_i^2 - \boldsymbol{R}_1^2\ n_i^1) \\ &= \min_{R_1^2} \sum_{i=1}^{n} (n_i^{2T}\ n_i^2 + n_i^{1T} n_i^1 - 2 n_i^{2T}\ \boldsymbol{R}_1^2\ n_i^1)\end{aligned} \tag{3}$$

In Eq. (3), the terms $n_i^{2T} n_i^{2T}$ and $n_i^1 n_i^1$ are always positive as they are the squared magnitudes of the n_i^2 and n_i^1 vectors, respectively. Therefore, to minimize the SSE in Eq. (3), the rotation matrix $\boldsymbol{R}_1^2$ has to be estimated in such a way to maximize the term $n_i^{2T} \boldsymbol{R}_1^2\ n_i^1$. One should note that because $\boldsymbol{R}_1^2\ n_i^1$ and n_i^2 are pointing in the same direction when dealing with compatible direction vectors, the term $n_i^{2T} \boldsymbol{R}_1^2\ n_i^1$ is always positive. This term can be formulated as the dot product in Eq. (4) and maximized using the quaternion approach proposed by Horn (1987), in which interested readers can find more details. The pertinent quaternion basics to this research are briefly explained here

$$\max_{R_1^2} \sum_{i=1}^{n} n_i^{2T} \boldsymbol{R}_1^2\ n_i^1 = \max_{R_1^2} \sum_{i=1}^{n} n_i^2 . \boldsymbol{R}_1^2\ n_i^1 \tag{4}$$

Quaternions have one real and three imaginary elements, which are denoted in this paper by the symbol (O). A unit quaternion $\dot{q}$ can represent any rotation in 3D space by a rotation angle around an axis, which is defined by the real and imaginary parts of the quaternion. According to quaternion properties, the rotation multiplication $\boldsymbol{R}_1^2\ n_i^1$ is equivalent to the quaternion multiplication $\dot{q} \dot{n}_i^1 \dot{q}^*$, where the unit quaternion $\dot{q}$ corresponds to $\boldsymbol{R}_1^2$, and $\dot{q}^*$ is the conjugate quaternion constructed by negating the imaginary part of $\dot{q}$. The term $\dot{n}_i^1$ is the quaternion form of n_i^1, which is nothing but adding a zero as the real part and the three elements of n_i^1 as the imaginary part, i.e., $n_i^1 = (0,\ n_i^1)$. Using quaternion properties, Eq. (4) can be rewritten as in Eq. (5), where $\boldsymbol{C}$ and $\overline{\boldsymbol{C}}$ are 4×4 matrices that convert the quaternion-based multiplication to a matrix-based multiplication, and the summation matrix $\boldsymbol{S}$ is a 4×4 matrix constructed using the components of n_i^1 and n_i^2 for all the available conjugate line pairs. To maximize the term $\dot{q}^T \boldsymbol{S} \dot{q}$ while maintaining the unity constraint of a quaternion rotation as represented in Eq. (6), one should use the Lagrange multiplier $\boldsymbol{\lambda}$ and maximize the target function φ in Eq. (7). To derive the desired quaternion, the target function φ should be differentiated with respect to $\dot{q}$, as seen in Eq. (8), which yields the expression in Eq. (9)

$$\begin{aligned}\max_{\dot{q}} \sum_{i=1}^{n} \dot{n}_i^2 . (\dot{q} \dot{n}_i^1 \dot{q}^*) &= \max_{\dot{q}} \sum_{i=1}^{n} (\dot{n}_i^2 \dot{q}) . (\dot{q} \dot{n}_i^1) \\ &= \max_{\dot{q}} \sum_{i=1}^{n} (C(\dot{n}_i^2) \dot{q}) . (\bar{C}(\dot{n}_i^1) \dot{q}) \\ &= \max_{\dot{q}} \sum_{i=1}^{n} \dot{q}^T C(\dot{n}_i^2)^T \bar{C}(\dot{n}_i^1) \dot{q} \\ &= \max_{\dot{q}} \dot{q}^T \Big(\sum_{i=1}^{n} C(\dot{n}_i^2)^T \bar{C}(\dot{n}_i^1) \Big) \dot{q} \\ &= \max_{\dot{q}} \dot{q}^T S \dot{q}\end{aligned} \tag{5}$$

$$\max_{\dot{q}} \dot{q}^T \boldsymbol{S} \dot{q},\ \ ||\dot{q}|| = 1 \tag{6}$$

$$\max_{\dot{q}} \varphi(\dot{q}) = \dot{q}^T \boldsymbol{S} \dot{q} - 2\boldsymbol{\lambda}(\dot{q}^T \dot{q} - 1) \tag{7}$$

$$\frac{\partial \varphi}{\partial \dot{q}} = 2\boldsymbol{S}\dot{q} - 2\boldsymbol{\lambda}\dot{q} = 0 \tag{8}$$

$$\boldsymbol{S}\dot{q} = \boldsymbol{\lambda}\dot{q} \tag{9}$$

The expression in Eq. (9) is satisfied if and only if $\boldsymbol{\lambda}$ and $\dot{q}$ are the corresponding eigenvalues and eigenvectors of the summation matrix $\boldsymbol{S}$. In this case, the term $\dot{q}^T \boldsymbol{S} \dot{q}$ would reduce to $\boldsymbol{\lambda}$, because the rotation defined by $\dot{q}$ is a unit quaternion [Eq. (10)]. Therefore, the term $\dot{q}^T \boldsymbol{S} \dot{q}$ is maximized when $\boldsymbol{\lambda}$ is the largest eigenvalue of the summation matrix $\boldsymbol{S}$, and eventually the unknown quaternion $\dot{q}$ is the eigenvector corresponding to the largest eigenvalue. The rotation matrix $\boldsymbol{R}_1^2$ and corresponding rotation angles (ω, φ, κ), if needed, can be derived from the quaternion $\dot{q}$ (Mikhail et al. 2001)

$$\dot{q}^T \boldsymbol{S} \dot{q} = \dot{q}^T \boldsymbol{\lambda} \dot{q} = \boldsymbol{\lambda} \dot{q}^T \dot{q} = \boldsymbol{\lambda} \tag{10}$$

Estimating the Rotation Matrix When Dealing with Incompatible Direction Vectors

Existing approaches for quaternion-based estimation of the rotation matrix relating two reference frames using conjugate direction vectors assume that these direction vectors are compatible (e.g., Horn 1987; Guan and Zhang 2011). Assuming that the direction vectors for the available conjugate pairs are consistently incompatible (i.e., the direction vectors for all the conjugate pairs are pointing in opposite directions following the application of the appropriate rotation matrix), the expression in Eq. (2) would change to the one in Eq. (11). Also, the SSE that should be minimized for all the involved n conjugate linear features will take the form in Eq. (12)

$$n_i^2 = -\boldsymbol{R}_1^2\ n_i^1 + \ e_i \ \equiv \ e_i = \ n_i^2 + \boldsymbol{R}_1^2\ n_i^1 \tag{11}$$

$$\min_{R_1^2} \sum_{i=1}^{n} e_i^T e_i = \min_{R_1^2} \sum_{i=1}^{n} (n_i^2 + R_1^2\ n_i^1)^T (n_i^2 + R_1^2\ n_i^1)$$

$$= \min_{R_1^2} \sum_{i=1}^{n} (n_i^{2T}\ n_i^2 + n_i^{1T} n_i^1 + 2 n_i^{2T} R_1^2\ n_i^1) \qquad (12)$$

Thus, minimizing the SSE would require the minimization of the term $n_i^{2T} \boldsymbol{R}_1^2\ n_i^1$. One should note that because $R_1^2\ n_i^1$ and n_i^2 are pointing in opposite directions, the term $n_i^{2T} \boldsymbol{R}_1^2\ n_i^1$ is always negative. Following the same derivation in the previous section, one can establish that the quaternion $\dot{q}$, which corresponds to the unknown rotation matrix, is the eigenvector corresponding to the smallest eigenvalue of the summation matrix $\boldsymbol{S}$, which is equivalent to $\sum_{i=1}^{n} \boldsymbol{C}(\dot{n_i^2})^T \overline{\boldsymbol{C}}(\dot{n_i^1})$.

In summary, the summation matrix $\boldsymbol{S}$, whose eigenvalues/eigenvectors will be investigated for the derivation of the unknown rotation matrix, when dealing with consistently compatible or incompatible direction vectors is the same. The only difference is that for conjugate pairs with compatible direction vectors, the quaternion rotation would be the eigenvector corresponding to largest eigenvalue. For conjugate pairs with consistently incompatible direction vectors, the quaternion rotation would be the eigenvector that corresponds to the smallest eigenvalue. This means that the derivation of the quaternion rotation for these scenarios would follow identical procedures with the exception of choosing two different eigenvectors of the same summation matrix $\boldsymbol{S}$. The challenge is what to do if one is dealing with conjugate pairs of linear features that might be partially compatible/incompatible. To address this challenge, one could follow one of the options below:

1. One can assume that manually identified conjugate linear features will be chosen in such a way that the direction vectors are compatible. The advantage of this approach is that there will be a straightforward approach for the estimation of the rotation matrix; i.e., the approach introduced in Horn 1987 and Guan and Zhang (2011). The disadvantage is that this approach would add another burden during the manual identification of conjugate features.
2. One can assume that the manually identified conjugate linear features can be either compatible (i.e., having unified directions for conjugate linear features in space after the alignment) or incompatible. The disadvantage of this option is that there has to be a slightly more complex model to address such ambiguity. However, the advantages would include easier implementation of the manual identification of conjugate features and flexibility in expanding the proposed semiautomated procedure to a fully automated one (i.e., the operator does not need to worry about defining unified directions for conjugate linear features). In this research, the second option will be followed and the proposed procedure is outlined in the next section.

Proposed Procedure

The conceptual basis of the proposed approach is using the minimum number of conjugate pairs of linear features, which are needed for the estimation of the rotation, scale, and shift parameters, while entertaining possible directional ambiguities in the derivation of the rotation matrix. Then, the estimated transformation parameters together with the remaining conjugate pairs are used to identify the correct/valid estimate for the transformation parameters. Once the correct solution has been identified, it will be used to ensure the compatibility of the direction vectors for all the conjugate linear features. Finally, all the linear features are used to derive the transformation parameters relating the two point clouds.

A 3D linear feature has four degrees of freedom (Roberts 1988). Therefore, a single straight line identified in two overlapping point clouds allows for the estimation of four transformation parameters, which are the two shifts across the line direction as well as the two rotation angles defined by the line direction (i.e., the angles defined by the azimuth and the pitch of the line). Two parallel linear features would allow for the estimation of the transformation parameters except for the shift along the direction of the linear features. Two intersecting linear features, on the other hand, would allow for the estimation of the transformation parameters except for the scale factor between the reference frames of the two point clouds. Therefore, a set of two pairs of conjugate linear features that are not coplanar is the minimum number of required pairs for the estimation of the transformation parameters. For accurate estimation of the transformation parameters, the angular deviation between the pair of lines in a given point cloud should be as close as possible to 90°, whereas the spatial separation should be as large as possible.

Having established the minimum number of conjugate linear features for estimating the transformation parameters, one has to focus on how to estimate the rotation matrix while considering possible ambiguities in the direction vectors. To illustrate the rationale of the proposed procedure, one can consider the possible scenario in Fig. 1, where n_i^1 and n_j^1 are two noncoplanar features in the first point cloud and n_i^2 and n_j^2 are the corresponding linear features in the second scan. In this case, given that a particular set of direction vectors for n_i^1 and n_j^1 are chosen (e.g., the one shown in the left column of Fig. 2), one can have four possible configurations of direction vectors for the corresponding pair in the second point cloud (e.g., the ones represented by the right four columns in Fig. 2). Not knowing which one of the possible four configurations is the correct one, all of them need to be considered to derive possible solutions for the rotation matrix assuming compatible direction vectors. Considering all these configurations would lead to four estimates of the rotation matrix. However, a closer look at these possible configurations will reveal the fact that the 1st and 2nd configurations as well as the 3rd and 4th configurations are consistently incompatible. In other words, considering the pair of linear features in the first point cloud (left column in Fig. 2) and the line pair represented by the 1st configuration as a possible conjugate pair, one could derive two solutions for the rotation matrix that correspond to the 1st and 2nd configurations while using the eigenvectors of the summation matrix $\boldsymbol{S}$ that correspond to the largest and smallest eigenvalues. In a similar fashion, the solutions that correspond to the 3rd and 4th configurations could be derived while considering the eigenvectors of the summation matrix resulting from associating the direction vectors in the first point cloud and the 3rd configuration in the second point cloud. In other words, the four possible solutions for the rotation matrix could be derived from two summation matrices. A reduction of the possible solutions can be achieved by selecting the direction vectors in the first point cloud in such a way that the cross-product of n_i^1 and n_j^1 is in the same direction of the common perpendicular from n_i^1 to n_j^1. The direction vectors in the second point cloud should be set in the same manner. Doing so will eliminate the 3rd and 4th configurations, because the cross-product of n_i^2 and n_j^2 points in the opposite direction of the common perpendicular from n_i^2 to n_j^2 for these configurations. Therefore, the two solutions for the rotation matrix could be derived while considering the eigenvectors of the summation matrix when dealing with the matching pair in the 1st configuration.

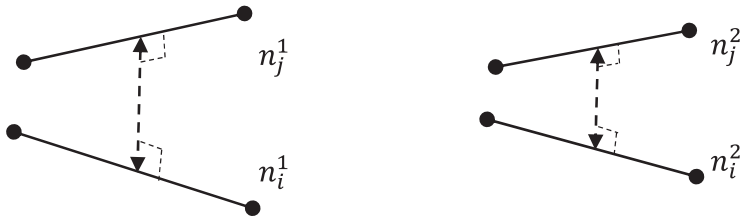

Fig. 1. Minimum linear feature requirement for the estimation of the transformation parameters relating two point clouds

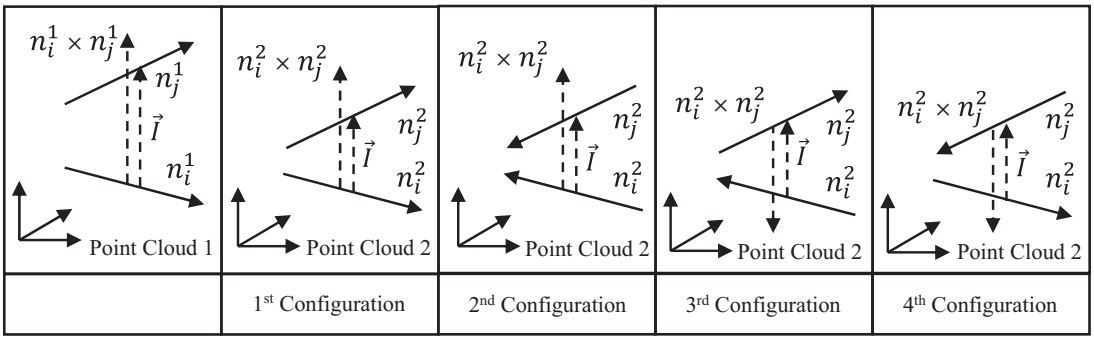

Fig. 2. Possible matching configurations between two pairs of conjugate linear features that are not coplanar

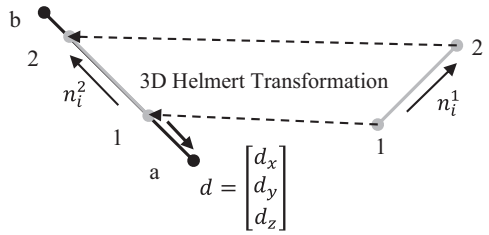

Fig. 3. Displacement vector for conjugate line segments with noncorresponding endpoints

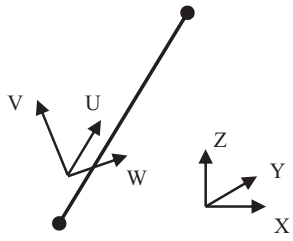

Fig. 4. Coordinate system for the point cloud *(X, Y, Z)* and the line local coordinate system *(U, V, W)*

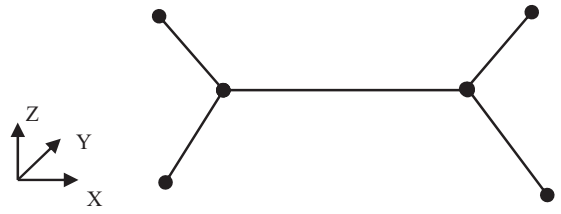

Fig. 5. Simulated linear features

Table 1. The 3D-Helmert Transformation Parameters Relating the Reference Frames for the Simulated Data Set

Parameter	Value
$T_X(m)$	26
$T_Y(m)$	−73
$T_Z(m)$	−139
S	2.5
ω°	34
ϕ°	−68
κ°	155

Estimation of Scale and Shift Parameters

Now that the procedure is established for deriving the possible solutions for the rotation matrix using the minimum number of required conjugate line pairs, it is time to focus on the estimation of the respective scale and shift parameters. First, start by assuming that the endpoints defining conjugate lines in the two point clouds are corresponding to each other. In this case, the mathematical model relating corresponding points in terms of the transformation parameters between the involved reference frames is provided in Eq. (13), where Points 1 and *a* in the first and second point clouds, respectively, are conjugate points along corresponding linear features. Given that there is a solution for the rotation matrix, the mathematical model would take the form in Eq. (14). The scale and shift parameters are linearly combined as seen in Eq. (15), which follows the traditional Gauss Markov model [Eq. (16)]. Assuming *n* conjugate lines, one would have 6*n* equations in four unknowns, which could be derived through least-squares adjustment as in (Eq. 17)

$$\begin{pmatrix} x_a \\ y_a \\ z_a \end{pmatrix} = \begin{bmatrix} x_T \\ y_T \\ z_T \end{bmatrix} + S\boldsymbol{R}_1^2 \begin{bmatrix} x_1 \\ y_1 \\ z_1 \end{bmatrix} + \begin{bmatrix} e_x \\ e_y \\ e_z \end{bmatrix} \text{ and } \begin{bmatrix} e_x \\ e_y \\ e_z \end{bmatrix} \sim (0,\ \sigma_o^2 \boldsymbol{P}^{-1}) \tag{13}$$

where $\begin{pmatrix} x_T & y_T & z_T \end{pmatrix}^T$ is the shift vector between the reference frames of the two point clouds; S is the scale factor; $\begin{pmatrix} e_x & e_y & e_y \end{pmatrix}^T$ is the random noise vector contaminating the observed point coordinates; and $\sigma_o^2 \boldsymbol{P}^{-1}$ is the variance-covariance matrix of the random noise vector

$$\begin{bmatrix} x_a \\ y_a \\ z_a \end{bmatrix} = \begin{bmatrix} x_T \\ y_T \\ z_T \end{bmatrix} + S \begin{bmatrix} x_1^2 \\ y_1^2 \\ z_1^2 \end{bmatrix} + \begin{bmatrix} e_x \\ e_y \\ e_z \end{bmatrix} \text{ where } \begin{bmatrix} x_1^2 \\ y_1^2 \\ z_1^2 \end{bmatrix} = \boldsymbol{R}_1^2 \begin{bmatrix} x_1 \\ y_1 \\ z_1 \end{bmatrix} \tag{14}$$

$$\begin{bmatrix} x_a \\ y_a \\ z_a \end{bmatrix} = \begin{bmatrix} x_1^2 & 1 & 0 & 0 \\ y_1^2 & 0 & 1 & 0 \\ z_1^2 & 0 & 0 & 1 \end{bmatrix} \begin{bmatrix} S \\ x_T \\ y_T \\ z_T \end{bmatrix} + \begin{bmatrix} e_x \\ e_y \\ e_z \end{bmatrix} \tag{15}$$

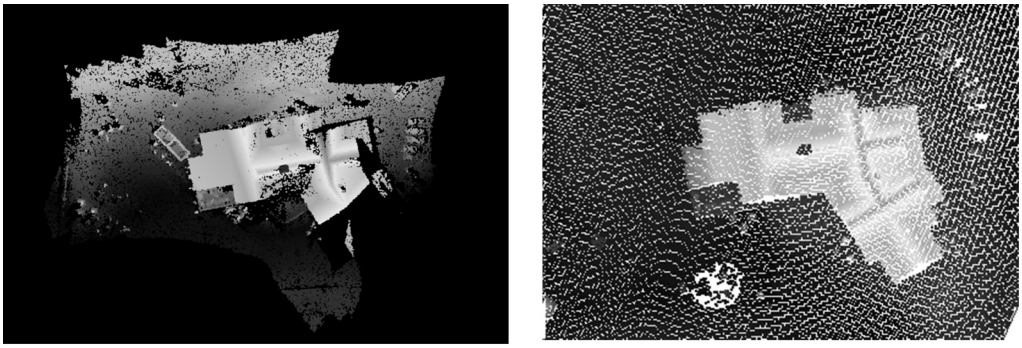

(a) (b)

Fig. 6. (a) Subsampled image-based point clouds that have been generated from UAV images; (b) airborne laser data over the test site (Real Data Set 1)

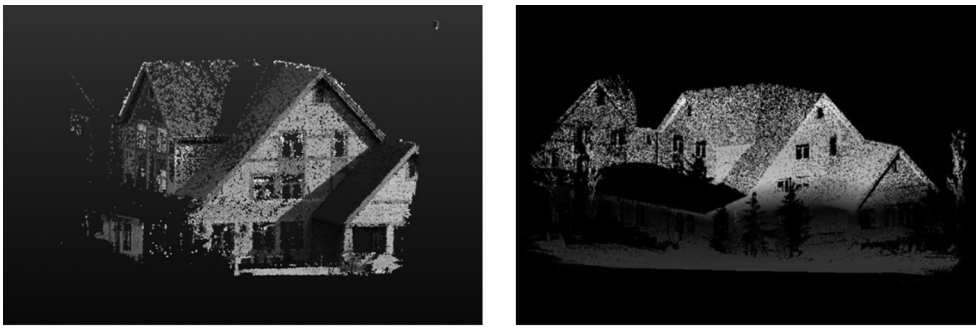

(a) (b)

Fig. 7. Subsampled point clouds that have been generated from: (a) a handheld Canon T3 camera; (b) a Faro Focus 3D laser scanner (Real Data Set 2)

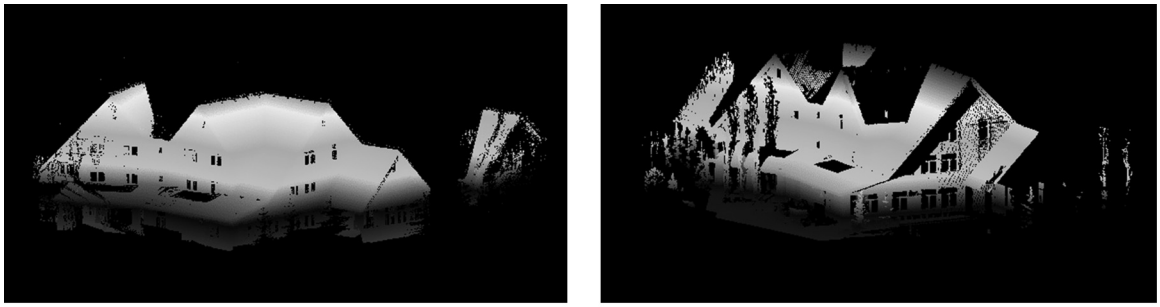

(a) (b)

Fig. 8. (a) Scan 1; (b) Scan 2 from a Faro Focus 3D scanner (Real Data Set 3)

$$y_{6n\times 1} = \boldsymbol{A}_{6n\times 4}\ x_{4\times 1} + e_{6n\times 1} \text{ and } e \sim (0,\ \sigma_o^2 P^{-1}_{6n\times 6n}) \tag{16}$$

$$\hat{x} = \left(\boldsymbol{A}^T\boldsymbol{P}\boldsymbol{A}\right)^{-1}\left(\boldsymbol{A}^T\boldsymbol{P}y\right) \tag{17}$$

Unfortunately, for the application at hand, conjugate direction vectors in the two point clouds are represented by their endpoints, which are not corresponding to each other. For example, one can consider the direction vector n_i^1 in the first point cloud, which is represented by the endpoints 1 and 2, and the corresponding direction vector n_i^2 in the second point cloud, which is represented by the endpoints a and b, where 1, 2 and a, b are not corresponding to each other (refer to Fig. 3). In this case, the mathematical model relating these points can be represented by Eq. (18). The main difference between Eqs. (13) and (18) is the displacement vector $\mathbf{d} = \begin{pmatrix} d_x & d_y & d_z \end{pmatrix}^T$. As seen in Fig. 3, the displacement vector is along the direction vector n_i^2. Eq. (18) can be reparameterized to the form in Eq. (19). The miss-closure vector in Eq. (19) $(\overline{e}_x, \overline{e}_y, \overline{e}_z)^T$ has two components. The first component $(e_x, e_y, e_z)^T$ is of a random nature, whereas the second component $(d_x, d_y, d_z)^T$is not random and is the result of dealing with noncorresponding points along conjugate linear features. Previous research has shown that the nonrandom component of the miss-closure vector can be eliminated by modifying the weight matrix according to Eq. (20) (Renaudin et al. 2011). Modifying the weight matrix will allow for the estimation of the transformation parameters in a similar manner to Eq. (17) after replacing the original weight matrix ($\boldsymbol{P}$) with the modified one ($\acute{\boldsymbol{P}}$). Refer to Renaudin et al. (2011) and Kersting et al. (2012) for more details regarding the underlying mathematical details of the weight modification approach

$$\begin{bmatrix} x_a \\ y_a \\ z_a \end{bmatrix} = \begin{bmatrix} x_T \\ y_T \\ z_T \end{bmatrix} + S\boldsymbol{R}_1^2 \begin{bmatrix} x_1 \\ y_1 \\ z_1 \end{bmatrix} + \begin{bmatrix} d_x \\ d_y \\ d_z \end{bmatrix} + \begin{bmatrix} e_x \\ e_y \\ e_z \end{bmatrix} \text{ and } \begin{bmatrix} e_x \\ e_y \\ e_z \end{bmatrix} \sim (0,\ \sigma_o^2 \boldsymbol{P}^{-1}) \tag{18}$$

$$\begin{bmatrix} x_a \\ y_a \\ z_a \end{bmatrix} = \begin{bmatrix} x_T \\ y_T \\ z_T \end{bmatrix} + S \begin{bmatrix} x_1^2 \\ y_1^2 \\ z_1^2 \end{bmatrix} + \begin{bmatrix} -e_x \\ -e_y \\ -e_z \end{bmatrix} \text{ where } \begin{bmatrix} -e_x \\ -e_y \\ -e_z \end{bmatrix} = \begin{bmatrix} e_x + d_x \\ e_y + d_y \\ e_z + d_z \end{bmatrix} \text{ and } \begin{bmatrix} -e_x \\ -e_y \\ -e_z \end{bmatrix} \sim (0,\ \sigma_o^2 \boldsymbol{P}^{-1}) \tag{19}$$

$$\acute{\boldsymbol{P}} \begin{bmatrix} d_x \\ d_y \\ d_z \end{bmatrix} = 0 \tag{20}$$

The weight-modification process is accomplished as follows:

1. For each of the direction vectors (n_i^2), one can derive a rotation matrix, $\boldsymbol{R}_{XYZ}^{UVW}$, which transforms the coordinates of a point from the reference frame of the second point cloud to a local coordinate system $(U,\ V,\ W)$, as illustrated in Fig. 4, where the U-axis is along the line direction.
2. The original weight matrix ($\boldsymbol{P}_{XYZ}$) is transformed from the XYZ coordinate system to the line local coordinate system ($\boldsymbol{P}_{UVW}$) according to the law of error propagation, as shown in Eq. (21)

$$\boldsymbol{P}_{UVW} = \boldsymbol{R}_{XYZ}^{UVW}\boldsymbol{P}_{XYZ}\boldsymbol{R}_{UVW}^{XYZ} \tag{21}$$

3. The weight matrix ($\boldsymbol{P}_{UVW}$) is modified according to Eq. (22). This modification can be conceptually explained as assigning a zero weight to discrepancies along the line direction

$$\boldsymbol{P}'_{UVW} = \begin{bmatrix} 0 & 0 & 0 \\ 0 & \boldsymbol{P}_V & \boldsymbol{P}_{VW} \\ 0 & \boldsymbol{P}_{WV} & \boldsymbol{P}_W \end{bmatrix} \tag{22}$$

4. Finally, the modified weight matrix can be transformed from the line local coordinate system to the reference frame of the second point cloud according to Eq. (23). This weight matrix will eliminate the impact of the displacement vector ($\vec{\mathbf{d}}$) from the miss-closure vector $(\overline{e}_x, \overline{e}_y, \overline{e}_z)^T$. Using such modified weight matrix, one could prove that the condition in Eq. (20) is satisfied

$$\boldsymbol{P}'_{XYZ} = \boldsymbol{R}_{UVW}^{XYZ}\,\boldsymbol{P}'_{UVW}\,\boldsymbol{R}_{XYZ}^{UVW} \tag{23}$$

Summary

In summary, the proposed procedure for the estimation of the transformation parameters in this work proceeds as follows:

Table 2. Number of Conjugate Line Pairs for the Three Real Data Sets

Real data set	Number of line pairs
1	7
2	8
3	10
4	10

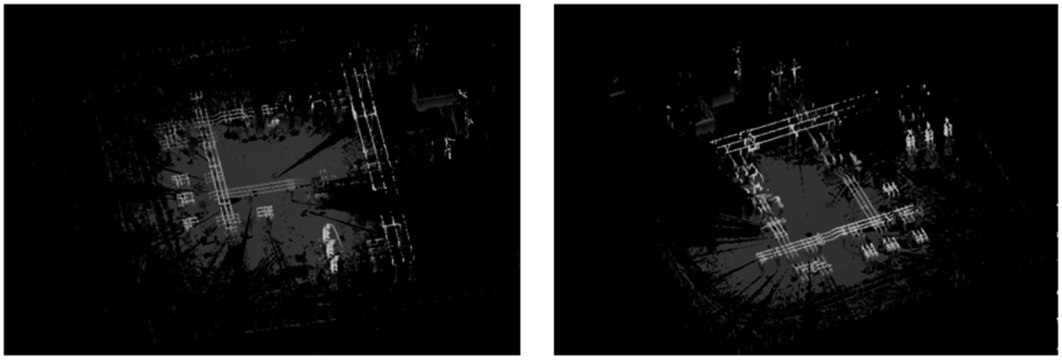

(a) (b)

Fig. 9. (a) Scan 1; (b) Scan 2 from the Faro Focus 3D scanner (Real Data Set 4)

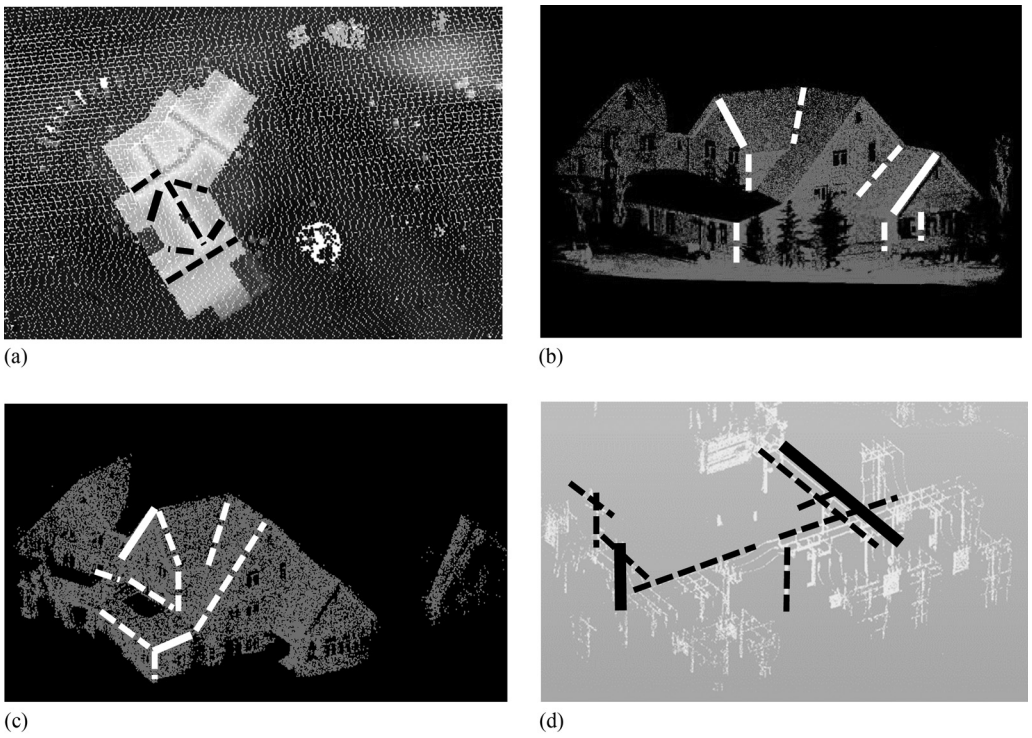

Fig. 10. Manually identified linear features in: (a) Data Set 1; (b) Data Set 2; (c) Data Set 3; (d) Data Set 4; the line pairs that have been used for the initial estimation of the transformation parameters are shown as solid lines; additional conjugate line pairs are displayed as dashed lines

1. Pick two pairs of conjugate linear features from the two point clouds. The linear features in a given point cloud should have large angular deviation (i.e., as close as possible to 90°) as well as spatial separation to ensure high-quality estimation of the transformation parameters.
2. Use these pairs to derive the two possible solutions for the rotation matrix relating the two point clouds as explained previously.
3. For each of the estimated rotation matrices, derive the corresponding scale and shift parameters as shown previously.
4. Using the estimated transformation parameters and the remaining pairs of conjugate linear features, it can be decided which one of these transformation parameters is the valid one. To do so, transform the endpoints of the linear features in the first point cloud to the reference frame of the second one. The valid solution will be the one that makes the linear features in the second reference frame and their transformed corresponding ones collinear for all the lines in the data set in question. The collinearity of the line segments in the second point cloud and the transformed ones from the first cloud will be checked through their spatial separation and angular deviation. More specifically, the spatial separation should be almost zero. whereas the angular deviation should be either close to 0° or 180°.
5. Having decided the valid solution, one proceeds by adjusting the direction vectors of the linear features to ensure that they are compatible. More specifically, after ensuring the collinearity of the linear features in the second reference frame and their transformed corresponding ones from the first point cloud, their direction vectors are adjusted to ensure that they are pointing in the same direction. In other words, if the angular deviation is almost 180°, the direction vector of one of the segments is inverted.
6. Using all the linear features, one estimates the rotation matrix according to the established procedure for the derivation of rotation matrix. Then, the estimated rotation matrix is used to derive the scale and shift parameters.
7. Finally, the ICPatch (Habib et al. 2010) is used for the fine registration between the involved point clouds.

Experimental Results and Discussions

Experimental results from simulated and real data sets have been conducted to investigate the capability of the proposed procedure in evaluating the scale, shift, and rotation parameters relating the reference frames of such data. The following subsections provide a brief overview of the utilized data sets, the estimated transformation parameters, and the visualization of the outcome of the registration process.

Data Set Description

Simulated Data Set

A set of five linear features have been simulated to emulate those arising from a gable roof building (Fig. 5). The longest line in this data set is less than 1 m. The linear features are represented by their endpoints. Then, a set of predefined 3D-Helmert transformation parameters (Table 1) is applied to these endpoints to generate the corresponding linear features in another reference frame. The endpoints of the transformed linear features are then manipulated to produce another set of endpoints to ensure that corresponding linear features are not represented by conjugate points. Finally, the order of the endpoints has been randomly changed to ensure that the linear features are not represented by compatible direction vectors.

Real Data Sets

The linear features for the real data sets have been derived from airborne and terrestrial passive and active sensors. Two test sites are involved in this research. The first one is at the vicinity of a building with a complex roof structure. The second one is around an electrical substation with sufficient polelike structures. More specifically, three different data sets (Data Sets 1–3) arising from the building and one data set (Data Set 4) arising from the electrical substation have been acquired. The following paragraphs provide the details pertaining to those data sets.

Data Set 1 is composed of two point clouds, which are generated from an image-based unmanned aerial vehicle (UAV) platform and an airborne laser scanner. The utilized UAV platform is the DJI Phantom 2 (DJI, Shenzhen China) equipped with a GoPro 3 camera (GoPro, San Mateo, California), which is used to capture 27 images. A total of 14 million points have been generated through the proposed approach for automated recovery of the image EOPs as well as the dense matching procedure. One should note that a local reference frame with an arbitrary scale factor has been established by the automated EOP recovery procedure. To reduce the processing time for the planar feature segmentation and derivation of linear features through an intersection procedure, the image-based point cloud has been subsampled to 100,000 points. The second point cloud in this data set is acquired by an Optech ALTM 3100 airborne laser scanning system (Teledyne Optech, Vaughan, Ontario, Canada). A total of 78,000 points that cover the building in question have been cropped from the airborne data. The average point spacing of the airborne data is about 0.75 m. Fig. 6 illustrates the subsampled image-based point cloud and the airborne laser data.

Data Set 2 has been generated from terrestrial platforms viewing some of the building facades. The first point cloud is generated from 21 digital images that were captured by a handheld Canon T3 camera (Canon Canada, Mississauga, Ontario, Canada). A total of 8 million points have been generated from the dense matching procedure. Similar to the first data set, these points have been subsampled to 60,000 points prior to the segmentation and linear feature derivation procedure. The second point cloud, which is composed of 1,140,000 points, is acquired by a Faro Focus 3D terrestrial laser scanner (Faro Technologies, Lake Mary, Florida). This data set is acquired to have a 2 cm resolution at a 15-m distance. The laser data is subsampled to 110,000 points. Fig. 7 illustrates the subsampled image-based and laser scanner point clouds.

Data Set 3 includes two point clouds acquired by the Faro Focus 3D scanner at two different locations. The main objective of this data set is to check the deviation of the estimated scale from the expected unit value. Fig. 8 illustrates the two point clouds, which are comprised of 360,000 and 1,140,000 points. To reduce the processing time for point cloud segmentation and linear feature extraction, the two scans are subsampled to 36,000 and 11,000 points, respectively.

Data Set 4 includes two point clouds acquired by the Faro Focus 3D scanner at two different locations within an electrical substation. Similar to Data Set 3, the main objective of this data set is to check the deviation of the estimated scale from the expected unit value. Fig. 9 illustrates these two point clouds, which are comprised of 11 million and 12 million points. To reduce the processing time for linear feature extraction, the two scans are subsampled to 55,000 and 60,000 points, respectively.

For Real Data Sets 1–3, the linear features have been extracted through the intersection of automatically segmented neighboring planar regions. For Real Data Set 4, the linear features have been extracted through direct region-growing segmentation. Conjugate linear features are then manually identified. Table 2 summarizes the number of manually identified conjugate linear features from each of the real data sets. Sketches illustrating the point clouds and extracted linear features from the different data sets are presented in Fig. 10, including the utilized line pairs for the initial estimation of the transformation parameters.

Table 3. Estimated Transformation Parameters from the Simulated Data Set with Different Noise Levels

Noise level (m)	$T_X(m)$	$T_Y(m)$	$T_Z(m)$	S	ω°	ϕ°	κ°
0.00	26	−73	139	2.50	34.00	−68.00	155.00
0.01	25.97	−73.01	139.02	2.45	33.78	−68.23	154.31
0.02	26.03	−72.98	138.97	2.46	33.79	−67.06	154.99
0.03	25.97	−73.01	139.02	2.52	34.29	−68.83	156.43
0.04	25.95	−72.98	139.01	2.51	36.88	−67.45	156.33
0.05	26.05	−72.97	138.95	2.42	32.07	−66.54	156.28

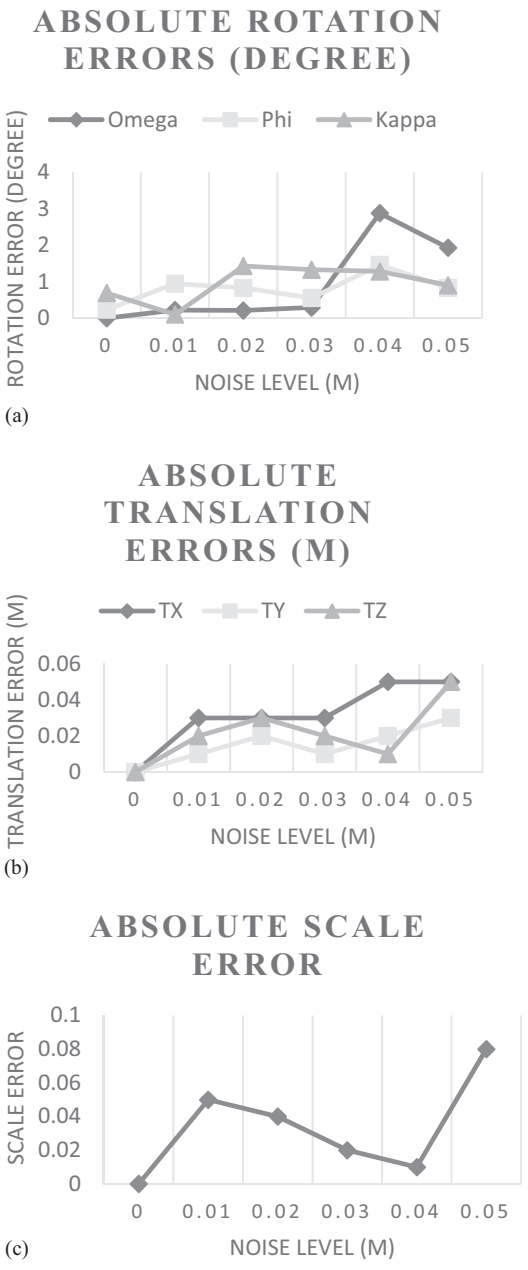

Fig. 11. (a) Rotation errors; (b) translation errors; (c) scale errors for the estimated transformation parameters from the simulated data sets with different noise levels

Results and Discussions

Simulated Data Set

The main objective of the simulated data set is to evaluate the estimated transformation parameters after adding noise with different magnitudes to the simulated endpoints of the linear features. Table 3 provides the estimated transformation parameters for these experiments. More specifically, the transformation parameters are derived through the proposed closed-form coarse-registration approach using the five conjugate linear features. As expected, in the absence of noise, the estimated transformation parameters are identical to those used to simulate the second data set. Fig. 11 illustrates the absolute values for the deviations between the estimated parameters and the corresponding true values for the different noise levels (i.e., noise with standard deviations from 0 to 0.05 m). As shown in Fig. 11, the maximum absolute error values for the translation, rotation angles, and scale factor are less than 0.0 5 m, 4°, and 0.1, respectively. Fig. 12 presents two examples of the postregistration alignment of the linear feature results, in which the Gaussian noise levels are 0.02 and 0.05 m, respectively. Based on these results, one can conclude that accurate coarse registration is achieved from the simulated data set, and the estimated transformation parameters are not significantly affected by the noise level in the endpoint coordinates. In this simulated data set, the length of linear features is similar to the size of the test region. Because the length of linear features is only important for determining the direction vectors, linear features with different lengths (e.g., shorter segments) would not affect the result of coarse registration. In other words, as long as the length of the linear features is sufficient for recovering the line direction vector, the coarse registration would

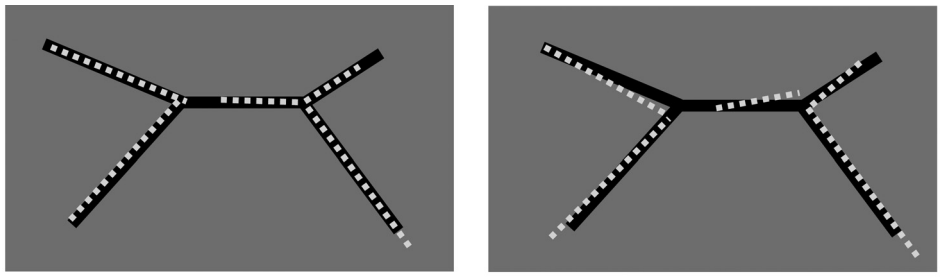

(a) (b)

Fig. 12. Postregistration aligned linear features from the simulated data set with noise level of: (a) 0.02 m; (b) 0.05 m; the original linear features are presented in solid lines, and the aligned linear features with different levels of Gaussian noise are shown as dashed lines

Table 4. Estimated Transformation Parameters from Real Data Sets 1–4

Data	Parameter source	$T_X(m)$	$T_Y(m)$	$T_Z(m)$	S	ω°	ϕ°	κ°
1	Initial	700121.46	5661856.18	1141.02	22.62	3.15	−3.72	111.02
	All lines	700121.11	5661852.73	1142.76	25.25	3.16	−6.06	111.62
	ICPatch	700121.25	5661851.68	1141.74	25.39	4.58	−5.52	111.74
2	Initial	−26.38	671.89	359.87	6.82	130.49	−62.31	34.41
	All lines	−19.46	680.02	364.34	4.38	125.97	−66.13	35.53
	ICPatch	−19.12	680.00	364.21	4.37	127.04	−65.50	34.98
3	Initial	−5.18	−12.58	−10.55	1.01	−0.04	−3.23	−52.36
	All lines	−4.98	−12.54	−10.07	1.00	0.22	−2.49	−52.42
	ICPatch	−4.80	−12.61	−9.96	1.00	0.43	−2.29	−52.21
4	Initial	1.99	−8.80	0.06	0.98	−0.13	−0.02	2.43
	All lines	1.92	−9.05	−0.06	1.00	0.15	0.02	2.39
	ICPatch	1.93	−9.00	−0.03	1.00	0.45	−0.22	2.51

Table 5. Differences among the Estimated Transformation Parameters for All Real Data Sets

	Absolute difference between initial and line-based transformation parameters		Absolute difference between initial and ICPatch-based transformation parameters		Absolute difference between line-based and ICPatch-based transformation parameters	
Parameters	Maximum	Minimum	Maximum	Minimum	Maximum	Minimum
$\Delta\omega^\circ$	4.52	0.11	3.45	0.47	1.32	0.21
$\Delta\phi^\circ$	3.82	0.04	3.19	0.20	0.63	0.20
$\Delta\kappa^\circ$	1.12	0.04	0.72	0.08	0.55	0.04
ΔS	2.63	0.01	2.77	0.01	0.14	0
$\Delta T_X(m)$	6.92	0.07	7.26	0.06	0.18	0.01
$\Delta T_Y(m)$	8.13	0.04	8.11	0.20	1.05	0.02
$\Delta T_Z(m)$	4.47	0.12	4.34	0.03	1.02	0.03

provide comparable values for the transformation parameters. The robustness against length is attributed to the fact that the weights only rely on the direction of the line and not its length.

Real Data Sets

Table 4 reports the estimated transformation parameters from the different stages of the proposed approach. More specifically, the first row for each data set represents the estimated transformation parameters from the initial conjugate pair, which was used to resolve the directional ambiguity among conjugate linear features (refer to the solid lines in Fig. 10). The second row, on the other hand, shows the derived transformation parameters using all the conjugate linear pairs. Finally, the third row provides the estimated parameters from the ICPatch procedure. As shown in Table 5, which shows the differences between the estimated transformation parameters in Table 4, one can observe the small differences between the line-based coarse registration and the ICPatch-based fine registration. Moreover, the first row in Table 4 for each of the data sets shows that even using a single pair of noncoplanar linear features is capable of providing a reasonable estimate of the transformation parameters. The maximum translation difference between the two-line–based registration and fine registration is 8.13 m, whereas the maximum rotation angle error is 4.52°. However, because such an initial estimation is only used to ensure the compatibility of the direction vectors for the conjugate linear features, these deviations will not affect the reliability of the final estimation of the transformation parameters. Looking at the reported results in Table 4, one can observe that the estimated scale factors for the third and the fourth data sets are almost unity, which is another indication of the ability of the proposed procedure for evaluating the transformation parameters. As an independent check, additional check lines in the real data sets are used to evaluate the coarse-registration quality. The derived overall weighted residuals for the check lines (this measure shows how well conjugate lines, which have not been used for parameter estimation, are aligned) are listed in Table 6, in which it can be seen that the coarse registration resulted in good coalignment of the check lines. More specifically, the overall weighted residuals are derived through the modified weight matrix as presented in the methodology section, which eliminates discrepancies along the line direction.

Table 6. Derived Overall Residuals for the Check Lines in Data Sets 1–4

Data set	Number of check lines	Overall residual (m)
Real Data Set 1	2	0.27
Real Data Set 2	2	0.13
Real Data Set 3	2	0.07
Real Data Set 4	2	0.04

For qualitative evaluation of the outcome from the registration process, Figs. 13–16 show cross sections of the aligned data sets after the coarse and fine registration for the four real data sets. It is evident from these figures that the two point clouds for the different real data sets are roughly aligned using the line-based transformation parameters, whereas more accurate alignment is achieved using the derived parameters from the ICPatch process. These results demonstrate that the line-based transformation parameters are more than sufficient for the coarse registration.

Conclusions and Recommendations for Future Work

This paper outlined a closed-form solution for the coarse registration of overlapping point clouds using linear features, which have been automatically extracted and manually matched in these point clouds. Corresponding linear features within the point clouds are not assumed to be represented by conjugate points. Linear features have been used for solving the coarse registration problem for several reasons. Among them, the possibility of deriving linear features from point clouds covering man-made environments as well as the possibility of determining the transformation parameters using only two noncoplanar linear features in each point cloud are the key advantages. The utilization of quaternions allowed for a closed-form evaluation of the rotation matrix, which in turn permitted a linear solution to the scale and shift parameters relating the reference frames of the point clouds. However, the fact that there might be directional ambiguities between corresponding linear features in the two point clouds will lead to having more than one plausible estimate for the rotation matrix. To overcome such a problem, the proposed procedure started with using the

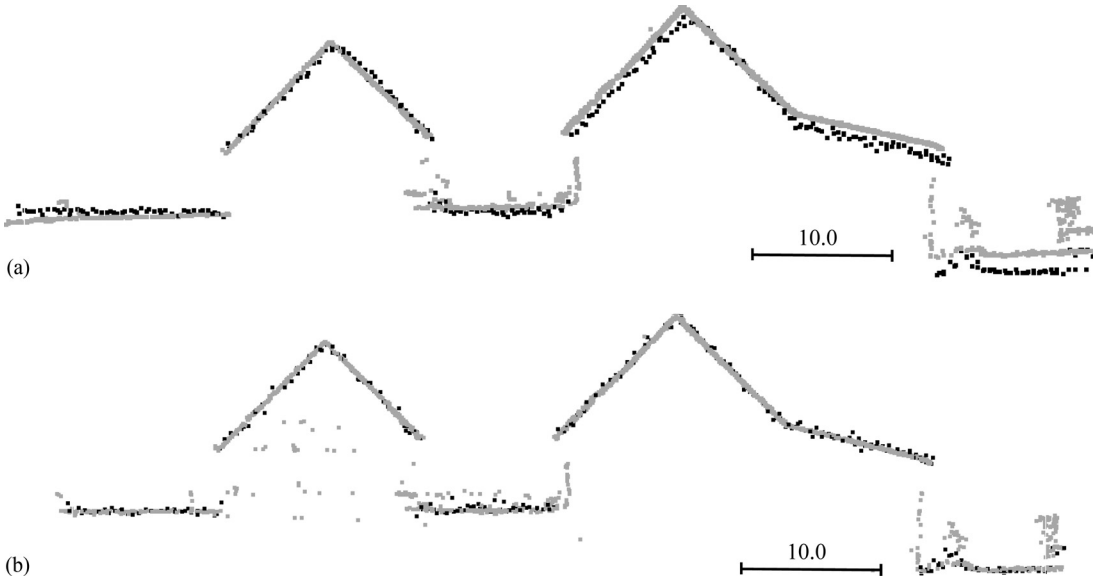

Fig. 13. Registration of Data Set 1: (a) coarse alignment using the line-based transformation parameters; (b) fine alignment using the ICPatch-based transformation parameters (the airborne laser scanning (ALS) data are shown in black, and the image-based point cloud is visualized in gray)

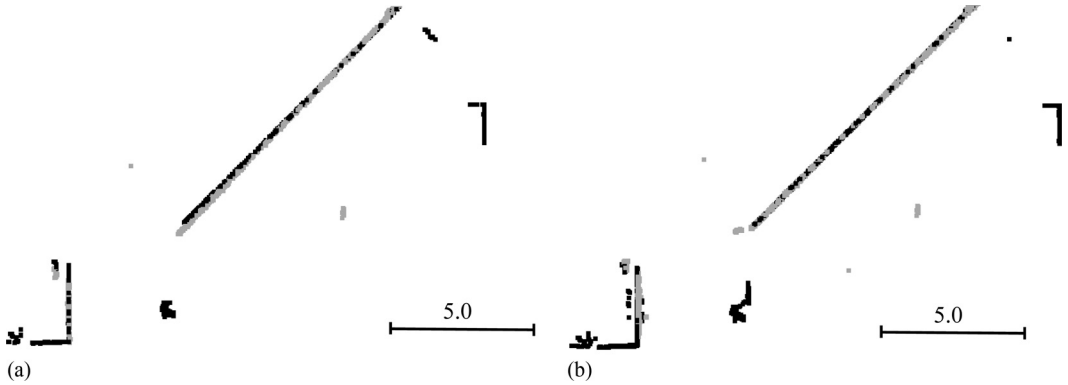

Fig. 14. Registration of Data Set 2: (a) coarse alignment using the line-based transformation parameters; b) fine alignment using the ICPatch-based transformation parameters (the terrestrial laser scanning (TLS) data are shown in black and the image-based point cloud is visualized in gray)

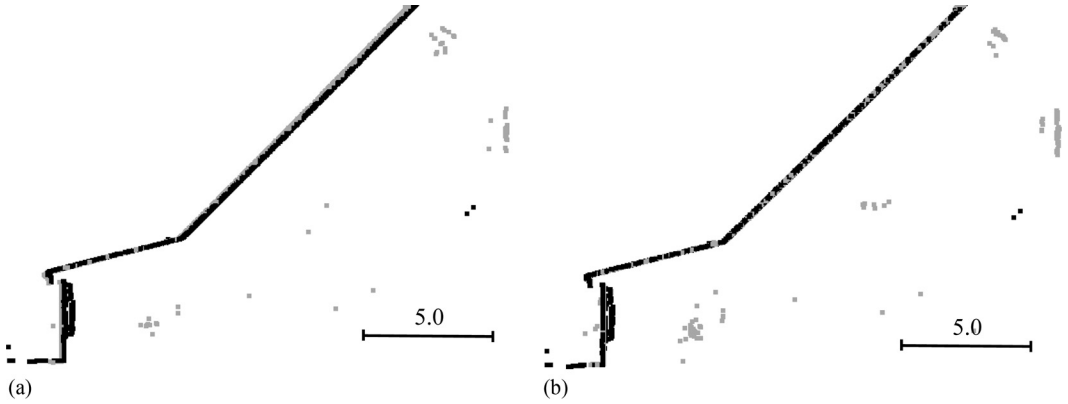

Fig. 15. Registration of Data Set 3: (a) coarse alignment using the line-based transformation parameters; (b) fine alignment using the ICPatch-based transformation parameters (the first TLS point cloud is shown in black and the second TLS point cloud is visualized in gray)

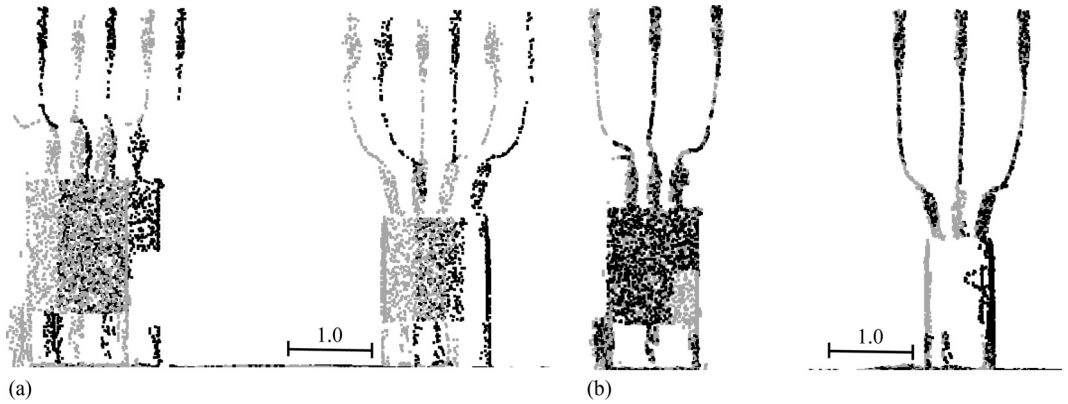

Fig. 16. Registration of Data Set 4: (a) coarse alignment using the line-based transformation parameters; (b) fine alignment using the ICPatch-based transformation parameters (the first TLS point cloud is shown in black and the second TLS point cloud is visualized in gray)

minimum number of required linear features for the estimation of the transformation parameters (i.e., two noncoplanar linear features in each point cloud) while allowing for multiple directional correspondences among the direction vectors for these linear features. This consideration leads to multiple solutions for the transformation parameters, which are then used for resolving the directional ambiguities between corresponding linear features. Then, all the available linear features are simultaneously used in the same manner to estimate the rotation matrix as well as scale and shift parameters. The proposed procedure has been tested with several simulated and real data sets, which verified the feasibility of the proposed procedure in terms of solving the registration problem in the presence of noisy measurements and providing reliable coarse alignment for a successful fine registration.

The main limitation of the proposed approach is the reliance on manual identification of corresponding linear features in the available point clouds. However, this could be achieved through a simply developed interactive visualization environment for the identification of these features among those that have been automatically extracted from the automated segmentation and intersection of neighboring planar features. The fact that the operator does not need to worry about ensuring the directional compatibility of the direction vectors would make this manual process even simpler. Having said that, current and future research will be focusing on the automated identification of corresponding linear features within the point clouds. A *RANSAC* procedure constrained by invariant characteristics relating conjugate linear features (e.g., similar angular deviations for any point clouds as well as similar spatial separation for point clouds sharing the same scale) would be used as the starting point for this automated procedure. In addition, the utilization of more than a single pair of linear features to reduce the number of required *RANSAC* trials also will be investigated. Moreover, future work will focus on the registration of more than two scans simultaneously while ensuring some sort of compatibility constraints among the transformation parameters relating multiple scans.

References

Al-Durgham, K., and Habib, A. (2014). "Association-matrix-based sample consensus approach for automated registration of terrestrial laser scans using linear features." *Photogramm. Eng. Remote Sens.*, 80(11), 1029–1039.

Besl, P. J., and McKay, N. D. (1992). "Method for registration of 3-D shapes." *Robotics-DL tentative*, International Society for Optics and Photonics, Bellingham, WA, 586–606.

Chen, C. C., and Stamos, I. (2006). "Range image registration based on circular features." *3D Data Processing, Visualization, and Transmission, Third Int. Symp.*, IEEE, New York, 543–550.

Chen, C.-S., Hung, Y.-P., and Cheng, J.-B. (1998). "A fast automatic method for registration of partially-overlapping range images." *Computer Vision, 1998, Sixth Int. Conf.*, IEEE, New York, 242–248.

Ding, M., Lyngbaek, K., and Zakhor, A. (2008). "Automatic registration of aerial imagery with untextured 3d lidar models." *Computer Vision and Pattern Recognition, 2008. CVPR 2008, IEEE Conf.*, IEEE, New York, 1–8.

Fischler, M. A., and Bolles, R. C. (1981). "Random sample consensus: A paradigm for model fitting with applications to image analysis and automated cartography." *Commun. ACM*, 24(6), 381–395.

Franaszek, M., Cheok, G. S., and Witzgall, C. (2009). "Fast automatic registration of range images from 3D imaging systems using sphere targets." *Automat. Construct.*, 18(3), 265–274.

Gehrke, S., Morin, K., Downey, M., Boehrer, N., and Fuchs, T. (2010). "Semi-global matching: An alternative to LIDAR for DSM generation." *Proc., 2010 Canadian Geomatics Conf. and Symp. of Commission*, International Archives of the Photogrammetry, Remote Sensing and Spatial Information Sciences, Calgary, Alberta, Canada, 38(B1), 15–18.

González-Aguilera, D., Rodríguez-Gonzálvez, P., and Gómez-Lahoz, J. (2009). "An automatic procedure for co-registration of terrestrial laser scanners and digital cameras." *J. Photogramm. Remote Sens.*, 64(3), 308–316.

Guan, Y., and Zhang, H. (2011). "Initial registration for point clouds based on linear features." *Knowledge Acquisition and Modeling (KAM), 2011 Fourth Int Symp.*, IEEE, New York, 474–477.

Habib, A., Detchev, I., and Bang, K. (2010). "A comparative analysis of two approaches for multiple-surface registration of irregular point clouds." *Proc., 2010 Canadian Geomatics Conf. and Symp. of Commission I*, International Archives of the Photogrammetry, Remote Sensing and Spatial Information Sciences, Calgary, Alberta, Canada, 38(part 1), 61–66.

Habib, A. F., and Alruzouq, R. I. (2004). "Line-based modified iterated Hough transform for automatic registration of multi-source imagery." *Photogramm. Rec.*, 19(105), 5–21.

Habib, A. F., Ghanma, M. S., and Tait, M. (2004). "Integration of LIDAR and photogrammetry for close range applications." *Proc., ISPRS XXth Conf.*, Istanbul, Turkey, 1045–1050.

Han, J.-Y. (2010). "A noniterative approach for the quick alignment of multistation unregistered LiDAR point clouds." *Geosci. Remote Sens. Lett., IEEE*, 7(4), 727–730.

Han, J.-Y., and Jaw, J.-J. (2013). "Solving a similarity transformation between two reference frames using hybrid geometric control features." *J. Chinese Inst. Eng.*, 36(3), 304–313.

He, F., and Habib, A. (2014). "Linear approach for initial recovery of the exterior orientation parameters of randomly captured images by low-cost mobile mapping systems." *Int. Arch. Photogramm. Remote Sens. Spatial Inf. Sci.*, XL-1, 149–154.

Hirschmuller, H. (2005). "Accurate and efficient stereo processing by semi-global matching and mutual information." *Computer Vision and Pattern Recognition, 2005, CVPR 2005, IEEE Computer Society Conf.*, IEEE, New York, 807–814.

Horn, B. K. (1987). "Closed-form solution of absolute orientation using unit quaternions." *J. Opt. Soc. Am. A*, 4(4), 629–642.

Huang, T. S., and Netravali, A. N. (1994). "Motion and structure from feature correspondences: A review." *Proc. IEEE*, 82(2), 252–268.

Jaw, J., and Chuang, T. (2008). "Feature-based registration of terrestrial lidar point clouds." *International society for photogrammetry and remote sensing, XXI congress, commission III. Processing of point clouds from laser scanners and other sensors*, J. Chen, J. Jiang, and H.-G. Mass, eds., International Archives of the Photogrammetry, Remote Sensing and Spatial Information Sciences, Beijing, China, 37, 303–308.

Kersting, A. P., Habib, A. F., Bang, K.-I., and Skaloud, J. (2012). "Automated approach for rigorous light detection and ranging system calibration without preprocessing and strict terrain coverage requirements." *Opt. Eng.*, 51(7), 076201-1.

Kim, H., and Hilton, A. (2013). "Evaluation of 3D feature descriptors for multi-modal data registration." 3DTV-Conf., 2013 Int. Conf., IEEE, New York, 119–126.

Kraus, K. (2007). *Photogrammetry: Geometry from images and laser scans*, Walter de Gruyter, New York.

Lari, Z., and Habib, A. (2013). "A novel hybrid approach for the extraction 907of linear/cylindrical features from laser scanning data." *ISPRS Ann. 908Photogramm. Remote Sens. Spatial Inf. Sci.*, 11-5-W2, 151–216.

Lari, Z., Habib, A. and Kwak, E. (2011). "An adaptive approach for segmentation of 3D laser point cloud." *ISPRS Workshop Laser Scanning*, Calgary, Canada, 29–31.

Mastin, A., Kepner, J., and Fisher, J. (2009). "Automatic registration of LIDAR and optical images of urban scenes." Computer Vision and Pattern Recognition, 2009, CVPR 2009, IEEE Conf., IEEE, New York, 2639–2646.

Matabosch, C., Salvi, J., Fofi, D., and Meriaudeau, F. (2005). "Range image registration for industrial inspection." Electronic Imaging 2005, International Society for Optics and Photonics, San Jose, CA, 216–227.

Mikhail, E. M., Bethel, J. S., and McGlone, J. C. (2001). *Introduction to modern photogrammetry*, Wiley, New York.

Remondino, F., and El-Hakim, S. (2006). "Image-based 3D modelling: A review." *Photogramm. Rec.*, 21(115), 269–291.

Renaudin, E., Habib, A., and Kersting, A. P. (2011). "Featured-based registration of terrestrial laser scans with minimum overlap using photogrammetric data." *ETRI J.*, 33(4), 517–527.

Roberts, K. S. (1988). "A new representation for a line." Computer Vision and Pattern Recognition, 1988. Proc., CVPR'88, Computer Society Conf., IEEE, New York, 635–640.

Rusinkiewicz, S., and Levoy, M. (2001). "Efficient variants of the ICP algorithm." 3-D digital imaging and modeling, 2001, Proc., Third Int. Conf., IEEE, New York, 145–152.

Slama, C. C., et al. (1980). *Manual of photogrammetry*, American Society of Photogrammetry, Falls Church, VA.

Stamos, I., and Leordeanu, M. (2003). "Automated feature-based range registration of urban scenes of large scale." Computer Vision and Pattern Recognition, 2003, Proc., 2003 IEEE Computer Society Conf., IEEE, New York, II–555.

Wolf, P. R., and Dewitt, B. A. (2000). *Elements of photogrammetry: With applications in GIS*, McGraw-Hill, New York.

Yao, J., Ruggeri, M. R., Taddei, P., and Sequeira, V. (2010). "Automatic scan registration using 3D linear and planar features." *3D Res.*, 1(3), 1–18.